

# Influence of modified light-flavor hadron spectra on particle yields in the statistical hadronization model

A. Andronic<sup>1</sup>, P. Braun-Munzinger<sup>2,3,4</sup>, D. Gündüz<sup>3</sup>,  
Y. Kirchoff<sup>3</sup>, M. K. Köhler<sup>3</sup>, J. Stachel<sup>2,3</sup>, and M. Winn<sup>5</sup>

<sup>1</sup> Institut für Kernphysik, Westfälische Wilhelms-Universität  
Münster, Münster, Germany

<sup>2</sup>Research Division and ExtreMe Matter Institute EMMI, GSI  
Helmholtzzentrum für Schwerionenforschung GmbH,  
Darmstadt, Germany

<sup>3</sup>Physikalisches Institut, Ruprecht-Karls-Universität  
Heidelberg, Heidelberg, Germany

<sup>4</sup>Institute of Particle Physics and Key Laboratory of Quark  
and Lepton Physics (MOE), Central China Normal University,  
Wuhan 430079, China

<sup>5</sup>Département de Physique Nucléaire (DPhN), Paris-Saclay  
Centre d'Etudes de Saclay (CEA), IRFU, Saclay, France

January 18, 2022

## Abstract

Hadron production in relativistic nuclear collisions is well described in the framework of the Statistical Hadronization Model (SHM). We investigate the influence on SHM predictions of hadron mass spectra for light-flavor baryons and mesons modified by the addition of about 500 new states as predicted by lattice QCD and a relativistic quark

model. The deterioration of the resulting thermodynamic fit quality obtained for Pb–Pb collision data at  $\sqrt{s_{\text{NN}}} = 2.76$  TeV suggests that the additional states are not suited to be naively used since also interactions among the states as well as non-resonant contributions need to be considered in the SHM approach. Incorporating these effects via the pion nucleon interaction determined from measured phase shifts leads again to excellent reproduction of the experimental data. This is a strong indication that at least the additional nucleon excited states cannot be understood and used as independent resonances.

## 1 Introduction

The wealth and precision of hadron-yield measurements in heavy-ion collisions at the LHC provide new insights into the hadronization process and the preceding collision stages. Within the framework of the statistical hadronization model (SHM) it can be shown that, under the assumption of a rapid chemical freeze-out of a thermalized medium, particle abundances are described by statistical weights with only a small set of parameters: the chemical freeze-out temperature  $T_{\text{CF}}$ , the baryo-chemical potential  $\mu_{\text{B}}$ , and the fireball volume  $V$  [1–7]. The particle species considered comprise the lightest and most abundantly produced hadrons such as pions as well as more complex and even loosely bound objects, such as (anti-)(hyper-)nuclei and all measured yields can be described with very good accuracy [6, 8]. The approach can also be extended to the heavy-flavor sector [6, 9, 10].

The SHM connects measurements of particle yields to the phase diagram of strongly interacting matter, which is resulting from Quantum-Chromodynamics (QCD). In particular, hadron production is governed by the QCD phase transition at a pseudo-critical temperature  $T_c$  between the Quark-Gluon Plasma (QGP), a state with quarks and gluons as degrees of freedom, and the confined phase where hadrons are the degrees of freedom [11]. The equations of QCD cannot be solved perturbatively for values of the strong coupling constant appropriate for typical particle distances and momentum transfers in the QGP. So far this can be done only numerically by putting the theory on a discretized space-time lattice in a method called lattice QCD (LQCD), see e.g. reference [12] for a recent review. An alternative is modelling QCD with effective field theories. The statistical operator emerging from LQCD studies is in fact in very good agreement with that

based on the hadron resonance gas approach and used in the analysis of hadron yields in the framework of the SHM, supporting the conjecture of quark-hadron duality close to the QCD phase boundary [6].

LQCD at zero temperature, as well as quark models with two or three constituent quarks, can be used for a prediction of baryon and meson mass spectra. These calculations can be confronted with experimental spectroscopic data to shed light on the degrees of freedom in the QCD mass spectrum.

In the SHM, the mass spectrum of hadronic states is needed to build the hadronic partition function. In previous investigations ([6] and references therein), the hadron mass spectrum was based entirely on experimental data as compiled by the Particle Data Group (PDG) [13]. The resulting mass spectrum is extraordinarily rich [14] and the density of states grows approximately exponentially up to the mass region of about 1.8 GeV, from where on the increase starts to flatten. This exponential growth was in fact predicted long ago [15] and led to the concept of a limiting temperature for hadronic matter. Incidentally, the value of  $T_{\text{CF}}$  obtained from SHM analyses is somewhat below this limiting temperature and, as demonstrated in [6], can be identified with the pseudo-critical transition temperature  $T_c$  between QGP and hadronic matter.

Above about 2 GeV, the states become very dense, the hadronic resonances start to strongly overlap and experimental identification becomes very difficult. The flattening of the experimentally known density of states at large mass prompted a study [4] to what extent the SHM predictions and fits of data would be influenced by missing states. Assuming a continued Hagedorn-type growth, an effect on the pion yield of up to 9 % was found. The experimental considerations just mentioned as well as comparison to LQCD predictions indicate that even in the mass range below 1.8 GeV the mass spectrum could be incomplete ([16] and references there). This has led to attempts [17], in the context of reconciling LQCD data on strangeness fluctuations with the HRG, to supplement the experimental data with theory input for the hadron mass spectrum. This input came, e.g., from LQCD [18, 19] as well as the relativistic quark model [20, 21]. A comparison of SHM predictions based on such a modified mass spectrum with data has not been made yet at the level of the first moments, i.e. the hadron yields. We note that, fortunately, the sensitivity to higher masses of SHM predictions for hadron yields is strongly reduced because the experimentally determined chemical freeze-out temperature  $T_{\text{CF}}$  is less than 160 MeV [6] and, hence, thermal pop-

ulation of hadrons with masses larger than 1.5 GeV is strongly Boltzmann suppressed. Nevertheless, since in these theoretical investigations many additional states are proposed, and some of them with large spin degeneracies, one should study their possible influence on hadron production in relativistic nuclear collisions. This is the aim of the present paper.

We conclude this introductory section with a remark that is becoming increasingly relevant as the SHM predictions are now tested with the LHC data at precisions well below the 10% level over a data range of more than 9 orders of magnitude. The case in point is the assumption, in the current formulation of the SHM, that the hadron mass spectrum can be obtained from the PDG compilation [13] of vacuum (zero temperature) experimental hadron masses and branching ratios. The successes reported in [6, 8] indeed lend strong experimental support to this assumption. This is, however, in stark contrast to predictions from LQCD [22, 23] and refs. there that hadron masses should change for small baryo-chemical potential as the temperature reaches values in the assumed cross over phase transition region. Yet, despite many experimental efforts, no convincing experimental evidence of any in-medium hadron mass change (apart from collisional broadening of the  $\rho$  meson, [24]) has been reported. The possibility of modified hadron masses in the SHM was analyzed in [25, 26]. There it was demonstrated that, to keep a good description of experimental data, scaling of masses necessitates a similar scaling of the chemical freeze-out temperature. This, however, is inconsistent with dropping masses as the temperature increases towards the (pseudo-)critical value.

Recently it was argued [27] that, at LHC energies, the chiral condensate effectively decouples from the thermal fireball, and relaxes quickly to the vacuum value, possibly leading to vacuum masses as employed in the SHM. However, in thermal equilibrium, such effects should be contained in the LQCD analysis.

A way out, however conflicting with LQCD predictions [28], could be that the phase transition is first order after all, but leads, directly below  $T_c$ , to a non-equilibrium state with vacuum masses that cannot be described under the complete equilibrium conditions of LQCD. Clearly, the absence of any firm experimental information on the order of the QCD phase transition is not satisfactory and calls for further experimental and theoretical investigations.

## 2 Model description

The description of the model given here is restricted to its basic features and focuses on the details of the hadronic states implemented in the SHM. A more detailed description of the model and the underlying assumptions can be found in [6] and references there.

The basic quantity for thermodynamic computations is the partition function  $Z(T, \mu, V)$ . For a hadron species  $i$  in the grand-canonical ensemble it can be written for an ideal (non-interacting) quantum gas in the following form<sup>1</sup>:

$$\ln Z_i = \frac{V g_i}{2\pi^2} \int_0^\infty \pm p^2 dp \ln (1 \pm \exp [-(E_i - \mu_i)/T]), \quad (1)$$

where  $g_i = 2(J_i + 1)$  is the degeneracy factor for the total angular momentum  $J$ ,  $p$  is the particle momentum, and  $E_i = \sqrt{p^2 + m_i^2}$  it's total energy. The sign (+) is for fermions and (-) for bosons. The chemical potential is given as  $\mu_i = \mu_B \cdot B_i + \mu_S \cdot S_i + \mu_{I3} \cdot I_{3i} + \mu_C \cdot C_i$ , where  $B$ ,  $S$ ,  $I_3$ , and  $C$  are the baryon, strangeness, 3-component of the isospin and charm quantum numbers.

From this partition function, the particle densities  $n_i$  and all thermodynamic quantities can be derived. In particular,

$$n_i(T, \mu_i) = N_i/V = -\frac{T}{V} \left( \frac{\partial \ln Z_i}{\partial \mu_i} \right)_{V,T} \quad (2)$$

$$= \frac{g_i}{2\pi^2} \int_0^\infty \frac{p^2 dp}{\exp [(E_i - \mu_i)/T] \pm 1}. \quad (3)$$

In addition, an eigenvolume correction may be applied in order to model repulsive interactions between different hadrons, as studied in detail in [29]. This leads to an iterative procedure for the consistent determination of the thermodynamic quantities. In particular, the particle densities are corrected by a common factor reducing all particle densities while yield ratios are, in general, unchanged. The impact of modeling interactions beyond this ansatz via the  $S$ -matrix approach [30] is discussed later in the context of the description of hadron yields with the modified particle spectra.

The total partition function of the model for  $T \lesssim T_{CF}$  can be written as

---

<sup>1</sup>Natural units,  $\hbar = c = k_B = 1$ , are used throughout this document.

a sum of mesonic and baryonic contributions:

$$\ln Z(T, \mu, V) = \sum_{i \in \text{mesons}} \ln Z_i(T, \mu_{I3}, \mu_S, \mu_C, V) + \sum_{i \in \text{baryons}} \ln Z_i(T, \mu_B, \mu_{I3}, \mu_S, \mu_C, V). \quad (4)$$

For comparison with experimental data, the particle yields are computed from the thermal densities  $n_i$  taking into account all strong decays. Starting from the thermal densities, decays are propagated via a decay matrix which gives statistical weights to the corresponding daughter particles incorporating the individual branching ratios. If the branching ratios for decays of a particle with mass  $m$  are not known, as is the case for particles introduced in this study on theoretical grounds but not established experimentally yet, the branching ratios are estimated based on the known systematics of the 500+ established hadrons and considering the decay phase space. For a hypothetical strong decay of the particle with mass  $m$  into a given final state with two daughter particles and a decay momentum  $|\mathbf{p}_1|$  the decay rate into the solid angle  $d\Omega$  can be written as [13]

$$d\Gamma = \frac{1}{32\pi^2} |\mathcal{M}|^2 \frac{|\mathbf{p}_1|}{m^2} d\Omega, \quad (5)$$

where  $\mathcal{M}$  is the Lorentz-invariant matrix element. Assuming that for competing strong decays of the hypothetical particle with mass  $m$  the genuine matrix element is typical for the strong decay and not different for different decay channels, we only consider the phase space factor to determine the branching ratios into different final states as given by the decay momenta. The decay channels considered are obtained from the known decays of hadrons with the same quantum numbers and considering the opening up of new allowed decay channels with increasing decay momentum. Taking into account only 2-body decays implies that we effectively treat all newly opening decays of states with unmeasured branching resonantly. A newly introduced  $\Delta$  resonance will decay partly via a lower-lying  $\Delta$  resonance as soon as energetically possible in addition to the direct decay to nucleon plus pion, which will in turn decay into nucleon plus pion thus effectively increasing the number of pions in the final state as phase space opens up. This is exactly what is measured for the known excited nucleon resonances. Similar arguments apply to the meson sector with intermediate  $\rho$  or  $\eta$  or  $K^*$  modes.

The particle list in the standard version of the SHM contains 555 established hadrons as given by the PDG [13]. This list of particles consists of 223 mesons (123 non-strange, 32 strange, 40 with charm, and 28 with beauty) and 270 baryons (104 non-strange, 96 strange, 56 with charm, and 14 with beauty). It includes, in addition, 62 nuclei, hyper-nuclei and anti-(hyper)-nuclei.

In the following, we discuss the impact of extending the hadron mass spectrum with particles expected from LQCD and the relativistic quark model.

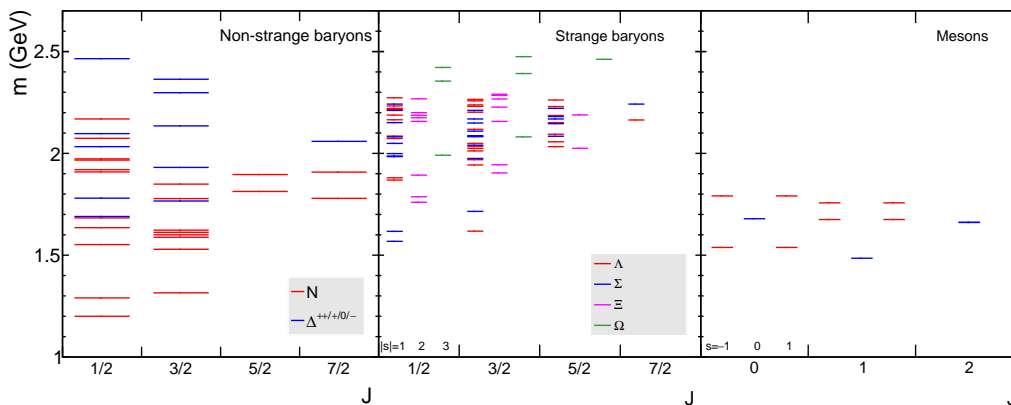


Figure 1: A synopsis of the additional states in terms of mass and total angular momentum for non-strange baryons (left panel), strange baryons (middle panel) and mesons (right panel).

### 3 Extension of the particle spectrum

Using theoretical input, the particle spectrum used in the SHM in this study is extended in 3 steps with respect to the original list based on experimentally established particles as given by the PDG [13]:

1. In a spectrum labelled 'udB' non-strange baryon states  $N^*$  with isospin  $I=1/2$  and  $\Delta^*$  with isospin  $I=3/2$  are added as predicted by a LQCD calculation [18]. Up to a mass of about 2.2 and 2.5 GeV, respectively, 23  $N^*$  doublets and 11  $\Delta^*$  quadruplets and the corresponding anti-baryons with total angular momenta between 1/2 and 7/2 have been added. The LQCD calculations have been performed with unphysically

massive light quarks resulting in pion masses between 396 and 524 MeV. Guided by the baryon mass evolution with decreasing light quark mass for the calculations shown in [18], we scale down the masses of the additional  $N^*$  and  $\Delta^*$  states from the LQCD results for  $m_\pi = 396$  MeV by a factor obtained comparing the masses of the already known non-strange baryon states. The scale factors are 0.71 and 0.76 for the  $N^*$  and  $\Delta^*$  states. Since several of the states are very closely spaced in mass, for convenience we group these states together in the code and adjust the corresponding degeneracy factors accordingly. This extension increases the number of non-strange baryons states from 104 to 284. The added states are visualized in the left panel of Fig. 1.

2. In a next step, in the spectrum labelled 'udsB', strange baryons are added as predicted in LQCD calculations by the same authors [19]. Also in these calculations, the light quark masses are unphysically high resulting in a pion mass  $m_\pi = 391$  MeV. In total 32  $\Lambda$  isospin singlets, 26  $\Sigma$  isospin triplets, 17  $\Xi$  isospin doublets and 7  $\Omega$  states as well as the according anti-baryons have been added. Following the same approach as chosen for the non-strange baryons, the mass spectra are scaled to the known states for the according multiplets, resulting in scaling factors 0.85, 0.88, 0.95 and 1.0 for the  $\Lambda$ ,  $\Sigma$ ,  $\Xi$ , and  $\Omega$  states, respectively. Due to the decreasing number of light valence quarks for the different isospin multiplets, it is plausible that scale factors approaching 1 are found with increasing strangeness. After scaling, an upper mass limit for the added baryons was chosen of 2.3 GeV for  $\Lambda$ ,  $\Sigma$ , and  $\Xi$  states and 2.5 GeV for  $\Omega$  states, resulting in the numbers of states given. In total the spectrum now contains 398 instead of originally 96 strange baryon states. The added states are shown in the middle panel of Fig. 1.
3. Finally, additional meson states are added. Since there is no LQCD result corresponding to the baryon predictions [18, 19], the spectrum 'udsBM' with added strange and non-strange meson states is based on a relativistic quark model [20]. In total 2 non-strange triplets, 2 non-strange singlets and 4  $K^*$  doublets and their anti-doublets are added. The mesons are added up to a mass limit of 1.7 GeV and 1.8 GeV for non-strange and strange multiplets, respectively. The increase in the total number of mesons is moderate, just about 10 %. The added states



are shown in the right panel of Fig. 1.

The decay matrix for the additional states is deduced from experimentally known states with the same quantum numbers as described above and considering a mass dependence due to the growing phase space with increasing mass as given in eq. 5.

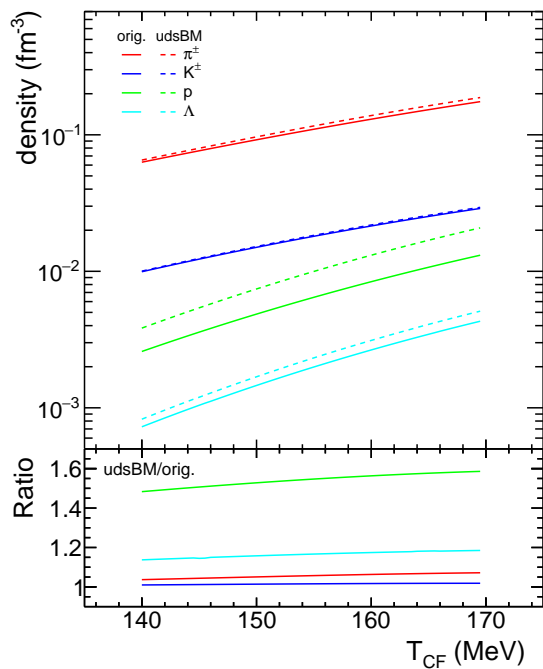


Figure 2: Temperature dependence of the thermal densities after strong decays for pions, kaons, protons, and  $\Lambda$  hyperons for the original (PDG) hadron spectrum and after the inclusion of the additional states (upper panel). The corresponding ratios are shown in the lower panel. The absolute values of the densities are for a calculation with an excluded volume parameter of 0.3 fm, to obtain values without excluded volume one needs to multiply by a factor 1.34.

The added states decay strongly into nucleons, the lightest strange baryons of a given strangeness, pions, and kaons. Correspondingly, the densities of those baryons and mesons change when new states are added and the change is temperature dependent, since with increasing  $T_{CF}$  temperature the added states

are populated increasingly. The temperature dependence of the thermal densities for pions, kaons, protons and  $\Lambda$  hyperons after strong decays (and electromagnetic decay of the  $\Sigma^0$ ) is shown in Fig. 2 for the original (PDG) hadron spectrum and after the inclusion of all additional states, corresponding to spectrum 'udsBM'.

While for the temperature range shown in Fig. 2 the effect on the pion density is very small (sub 10 %) and even less for the kaons, for the protons a significant increase in density of 50 to 60 % is observed due to the additional states. The large increase is due to the addition of some very low mass  $N^*$  resonances resulting from the LQCD calculation. They appear well below the Roper resonance ( $N^*(1440)$ ). For the  $\Lambda$  hyperons, the increase is smaller but not negligible with 15 to 20 %.

## 4 Resulting thermal fits

In this section we confront the SHM predictions using the modified hadron spectra to experimental hadron yields from the LHC. In analogy to the thermal fit discussed in [1], we perform fits based on a minimization of the  $\chi^2$  value between experimental hadron yields at mid-rapidity and SHM results varying the 3 free parameters. Here we use the ALICE data for Pb-Pb collisions at a collision energy per colliding nucleon pair of  $\sqrt{s_{NN}} = 2.76$  TeV. Experimental results for 22 particle species are used in the fits [31–37]. Effectively, there is only one free fit parameter to reproduce the yields of identified hadrons, the chemical freeze-out temperature  $T_{CF}$ , because for this collision system the baryon chemical potential is consistent with zero in all fits and the volume is fixed already by the overall charged particle multiplicity. Fit results for the original and the 3 modified hadron spectra are shown in Fig. 3 together with the experimental data. Using the original (PDG) hadron spectrum leads to results identical to the calculations reported in [6].

To allow a better visual comparison between the experimental data and the different thermal fits, the corresponding ratios for all fits are shown in Fig. 4. The experimental data points are well described in case of the original PDG particle list. In contrast, a significant and systematic deviation between data and calculations is observed when using the modified hadron mass spectra.

Both figures show clear modifications for all particle species between the original fit and the fits with modified hadron spectra. The 3 fits with addi-

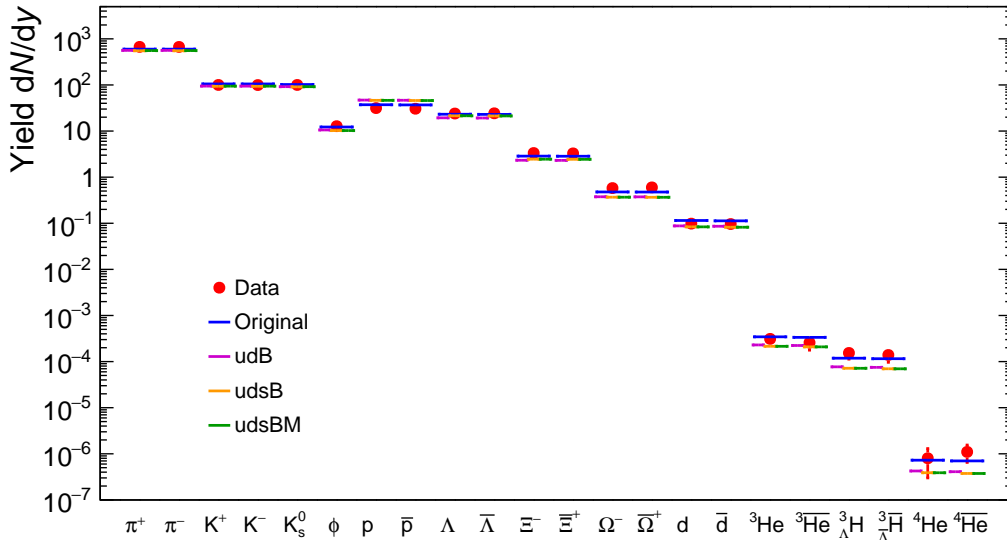


Figure 3: Comparison of particle yields measured by ALICE at mid-rapidity (references see text) to the fit using the original (PDG) spectrum and model fits using the 3 modified hadron spectra.

tional states group together for most particle species, with the exception of the strange baryon sector, where the fit using the spectrum 'udB' shows the largest discrepancy to the original fit result, while using the spectra 'udsB' and 'udsBM' represents an improvement, in particular for the  $\Lambda$ . The key to this observation is already visible in Fig. 2. Adding the additional states *increases* the proton yield in the model. However, already using the original PDG hadron spectrum results in a proton yield high by about 15 % compared to experimental data. Incidentally, this deviation from the experimental data by 2.6 standard deviations is the only significant discrepancy between data and model with the original PDG spectrum (and in the absence of the S-matrix correction, see below). Therefore it is immediately clear that a further increase in the model proton yield can only lead to significant deterioration since the proton yield is measured with high precision. In line with this observation, with the additional states the proton discrepancy grows and drives the fit to a smaller temperature to mitigate in part the detrimental effect of an increased proton yield, still yielding a larger than 30 % deviation for the proton yield. The drop in temperature is 3.5 MeV for spectrum 'udB'

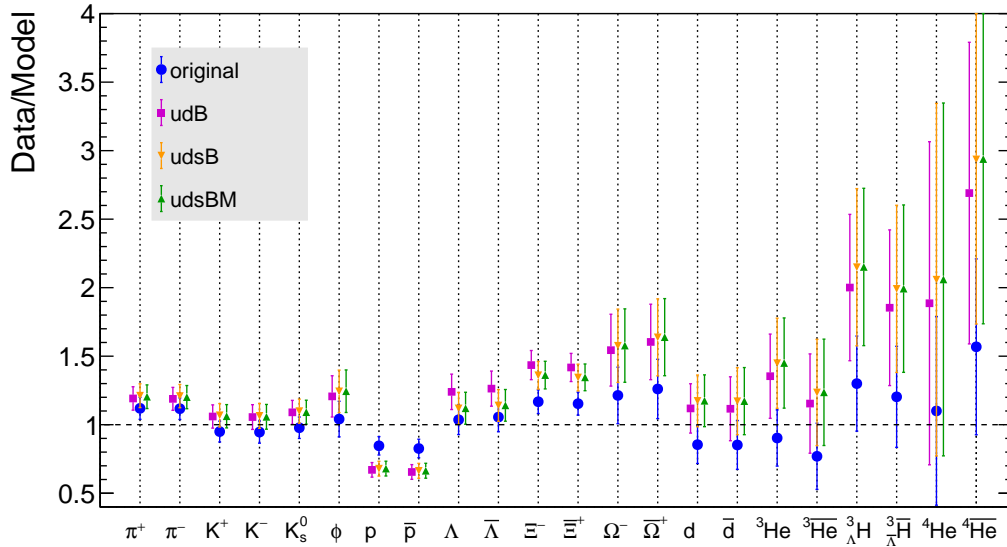


Figure 4: Ratio of ALICE experimental data over model fit for yields of all 22 fitted particle species for the original and the 3 modified hadron spectra.

and 4 MeV for spectra 'udsB' and 'udsBM'. Due to this drop in temperature, the yields for all other hadrons start to differ significantly, as visible in Fig. 4. With the temperature in the model fit reduced, all yields other than the protons are under-predicted more or less significantly.

In order to illustrate this effect quantitatively, we show in Fig. 5 the values of the chemical freeze-out temperature  $T_{\text{CF}}$  obtained from the four different fits, and the corresponding  $\chi^2/N_{\text{dof}}$  values. The freeze-out temperature values from the thermal fits decrease from 156.5 MeV for the original PDG hadron spectrum by about 4 MeV for the fits with modified mass spectra. The fit uncertainty of 1.5 MeV is indicated for the original PDG spectrum fit. For all spectra the fit uncertainty is strongly correlated and the drop is significant. On the other hand, the reduced  $\chi^2$  increases from 1.6 to a value of about 8 for the 'udB' mass spectrum where  $N^*$  and  $\Delta^*$  resonances are added, to drop again slightly to a value a bit above 7 when strange baryons and mesons are also added with the 'udsB' and 'udsBM' mass spectra.

As can be seen in Fig. 1, there are three  $N^*$  states which have masses significantly lower than the other baryons and well below the lightest known isospin 1/2 excitation, the  $N^*(1440)$ . Already the low mass of the Roper res-

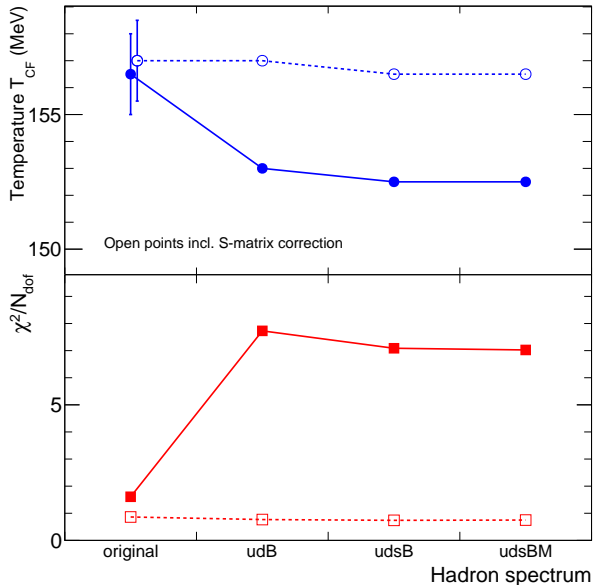


Figure 5: Chemical freeze-out temperature  $T_{\text{CF}}$  (upper panel) and  $\chi^2/N_{\text{dof}}$  (lower panel) for the 4 different model fits (solid symbols). The spectrum used is indicated as the x-axis label. S-matrix corrected values are shown as open points. The error bars indicate the uncertainty of the fitted temperature for the original PDG spectrum.

onance as first radial excitation of the nucleon together with its electromagnetic form factor has been a long standing puzzle only resolved recently [38]. It is all the more surprising to find significantly lower isospin  $1/2$  excitations with  $J^\pi = 1/2^-$  and  $3/2^-$ . We also note here that, in the baryon spectrum from the constituent quark model [21], such low-lying nucleon resonances do not arise. As a cross check, these three states were removed to evaluate their impact on the thermal fits. Indeed the effect on the fit result and quality is significant: the fitted temperature rises by 2 MeV and the  $\chi^2/N_{\text{dof}}$  drops from 7.15 to 4.3.

Concurrently to the present study, an approach, which takes into account the pion-nucleon interaction through the  $S$ -matrix formalism [30] was applied successfully to properly reproduce the measured proton abundance at LHC energy using the original PDG hadron spectrum [39]. This approach resulted in a moderate, temperature dependent reduction of the computed proton yield, e.g. by about 17 % at  $T_{\text{CF}} = 156.5$  MeV. This brought the com-

puted proton yield completely in line with the experimental data, resulting in a thermal fit with a reduced  $\chi^2$  value of 16.9/19, without change in the fit temperature. This approach effectively resolved the only significant discrepancy between model predictions and data, leading to an excellent description of all experimental results.

To benefit from the recognition, in refs. [30, 39], that taking into account via the  $S$ -matrix approach non-resonant and repulsive components in the pion-nucleon interaction for some partial waves leads to a much improved description of the SHM proton yields, this approach is also tested for the current modified hadron spectra with additional states. We apply during the fitting procedure with each of the 4 hadron spectra the appropriate correction to the proton yield as computed in [39]. The results are also displayed in Fig. 5 by the open symbols. As reported in [39], for the original PDG hadron spectrum the resulting fit temperature is practically unchanged but the reduced  $\chi^2$  value drops from 29/19  $\approx$  1.5 to 16.9/19  $\approx$  0.9. Also for the modified spectra with the additional states, this results in a dramatic improvement compared to fits without this  $S$ -matrix correction. Comparing the fit based on the PDG spectrum to the one with the 180 additional nucleon excitations (spectrum 'udB'), the fit result and quality are identical. The statistical model fit yields identical results with or without the additional excited nucleon states.

That implies that, after properly taking into account the pion-nucleon interaction via the measured phase shifts and the according  $S$ -matrix correction to the chiral susceptibilities and the pressure, there is obviously no room for additional independent resonant contributions. It is just as if these states did not exist. They leave no trace in the phase shifts and virial expansion of the interaction contribution to the pressure in the hadron resonance gas model. Inspecting the phase shifts for the partial waves corresponding to the low lying additional  $N^*$  resonances that have the largest effect on the proton yields computed without  $S$ -matrix correction, i.e. the S11 and D13 for the  $J^\pi = 1/2^-$  and  $3/2^-$  states given in [30], there is no indication for any other resonant contribution. The integrated contribution of both the S11 and D13 partial waves to the chiral susceptibility is about 30 % less than the naive resonance contribution for the PDG states [30] and consequently even less for a spectrum with additional states of these quantum numbers. Similar conclusions can be drawn for the other additional states vis-a-vis the partial wave analysis. For the partial waves corresponding to  $\Delta 1/2^-, 1/2^+, 3/2^-, 5/2^-, 5/2^+$  and the  $N^* 3/2^+$  the contribution to the chi-

ral susceptibility is negative, corresponding to repulsion in the respective  $\pi N$  channel. This is not to say these additional states do not exist, they may well. The phase shift analysis and S-wave correction to the hadron resonance gas (SHM) tell us that they should not be treated as independent resonances. When coupled to the continuum they could strongly rearrange, inducing non-resonant or repulsive interactions [40].

For the spectra with additional strange baryons and additional mesons the fits with  $S$ -matrix correction for the pion-nucleon interaction are even slightly better as can be seen in Fig. 5. The currently available  $S$ -matrix correction does not affect the yields of strange baryons and we currently have no information on the effect of the pion-hyperon interaction on the SHM predictions.

## 5 Summary and conclusion

We presented results of thermal fits to hadron yields measured at the LHC in central Pb–Pb collisions, performed in the statistical hadronization approach including additional baryon and meson states proposed by LQCD calculations and a relativistic constituent quark model. Adding these additional states to those obtained from the PDG compilation leads to a strong deterioration of the thermal fit quality as well as to a reduction of the chemical freeze-out temperature by about 4 MeV. The deterioration is driven entirely by the added non-strange baryons, the  $N^*$  and  $\Delta^*$  states. The application of the  $S$ -matrix correction completely restores the quality of the SHM fit with resulting temperature very close to 156.5 MeV.

These results indicate that the additional excited nucleon states, if they exist, are not realized in nature as independent resonances. In any case, the  $S$ -matrix treatment of the pion-nucleon interaction contains the complete physical information and should be appropriate for any spectrum as long as all of the corresponding partial waves for the quantum numbers of the states used are included. The outcome of this study is twofold. The added excited nucleon states  $N^*$  and  $\Delta^*$  do not leave any trace in the thermal fits of the LHC data after  $S$ -matrix correction for the pion-nucleon interaction. The addition of a large number of excited hyperons and of some non-strange and strange mesons gives slightly improved fits to experimental yields. The effect on the extracted chemical freeze-out temperature is negligible. Both observations show that the extraction of chemical freeze-out parameters from

the first moments of hadron multiplicities, the event averaged yields, is rather robust against addition of even a large number of hadronic states. Whether this is the case also for SHM analysis of higher moments is currently a matter of debate [41–43].

## 6 Acknowledgement

We would like to thank Pok Man Lo and Krzysztof Redlich for enlightening discussions. This work was funded in part by the DFG (German Research Foundation) – Project-ID 273811115 – SFB1225/ISOQUANT.

## References

- [1] A. Andronic, P. Braun-Munzinger, and J. Stachel, “Hadron production in central nucleus-nucleus collisions at chemical freeze-out,” *Nucl. Phys. A* **772** (2006) 167–199, [arXiv:nucl-th/0511071](#) [nucl-th].
- [2] F. Becattini, J. Manninen, and M. Gazdzicki, “Energy and system size dependence of chemical freeze-out in relativistic nuclear collisions,” *Phys. Rev. C* **73** (2006) 044905, [arXiv:hep-ph/0511092](#).
- [3] J. Cleymans, H. Oeschler, K. Redlich, and S. Wheaton, “Status of chemical freeze-out,” *J. Phys. G* **32** (2006) S165–S170, [arXiv:hep-ph/0607164](#).
- [4] A. Andronic, P. Braun-Munzinger, and J. Stachel, “Thermal hadron production in relativistic nuclear collisions: The Hadron mass spectrum, the horn, and the QCD phase transition,” *Phys. Lett. B* **673** (2009) 142–145, [arXiv:0812.1186](#) [nucl-th]. [Erratum: *Phys. Lett. B* **678** (2009) 516].
- [5] M. Floris, “Hadron yields and the phase diagram of strongly interacting matter,” *Nucl. Phys. A* **931** (2014) 103–112, [arXiv:1408.6403](#) [nucl-ex].
- [6] A. Andronic, P. Braun-Munzinger, K. Redlich, and J. Stachel, “Decoding the phase structure of QCD via particle production at high energy,” *Nature* **561** (2018) 321–330, [arXiv:1710.09425](#) [nucl-th].



- [7] V. Vovchenko, B. Dönigus, and H. Stoecker, “Canonical statistical model analysis of p-p , p -Pb, and Pb-Pb collisions at energies available at the CERN Large Hadron Collider,” *Phys. Rev. C* **100** (2019) 054906, [arXiv:1906.03145 \[hep-ph\]](#).
- [8] P. Braun-Munzinger and B. Dönigus, “Loosely-bound objects produced in nuclear collisions at the LHC,” *Nucl. Phys. A* **987** (2019) 144–201, [arXiv:1809.04681 \[nucl-ex\]](#).
- [9] P. Braun-Munzinger and J. Stachel, “(Non)thermal aspects of charmonium production and a new look at J / psi suppression,” *Phys. Lett. B* **490** (2000) 196–202, [arXiv:nucl-th/0007059 \[nucl-th\]](#).
- [10] A. Andronic, P. Braun-Munzinger, M. K. Köhler, K. Redlich, and J. Stachel, “Transverse momentum distributions of charmonium states with the statistical hadronization model,” *Phys. Lett. B* **797** (2019) 134836, [arXiv:1901.09200 \[nucl-th\]](#).
- [11] P. Braun-Munzinger and J. Wambach, “The Phase Diagram of Strongly-Interacting Matter,” *Rev. Mod. Phys.* **81** (2009) 1031–1050, [arXiv:0801.4256 \[hep-ph\]](#).
- [12] C. Ratti, “Lattice QCD and heavy ion collisions: a review of recent progress,” *Rept. Prog. Phys.* **81** (2018) 084301, [arXiv:1804.07810 \[hep-lat\]](#).
- [13] **Particle Data Group** Collaboration, M. Tanabashi *et al.*, “Review of particle physics,” *Phys. Rev. D* **98** (2018) 030001.
- [14] M. F. M. Lutz *et al.*, “Resonances in QCD,” *Nucl. Phys. A* **948** (2016) 93–105, [arXiv:1511.09353 \[hep-ph\]](#).
- [15] R. Hagedorn, “Statistical thermodynamics of strong interactions at high-energies,” *Nuovo Cim. Suppl.* **3** (1965) 147–186.
- [16] P. M. Lo, M. Marczenko, K. Redlich, and C. Sasaki, “Matching the Hagedorn mass spectrum with Lattice QCD results,” *Phys. Rev. C* **92** (2015) 055206, [arXiv:1507.06398 \[nucl-th\]](#).
- [17] A. Bazavov *et al.*, “Additional Strange Hadrons from QCD Thermodynamics and Strangeness Freezeout in Heavy Ion Collisions,” *Phys. Rev. Lett.* **113** (2014) 072001, [arXiv:1404.6511 \[hep-lat\]](#).

- [18] R. G. Edwards, J. J. Dudek, D. G. Richards, and S. J. Wallace, “Excited state baryon spectroscopy from lattice QCD,” *Phys. Rev. D* **84** (2011) 074508, [arXiv:1104.5152 \[hep-ph\]](#).
- [19] **Hadron Spectrum** Collaboration, R. G. Edwards, N. Mathur, D. G. Richards, and S. J. Wallace, “Flavor structure of the excited baryon spectra from lattice QCD,” *Phys. Rev. D* **87** (2013) 054506, [arXiv:1212.5236 \[hep-ph\]](#).
- [20] D. Ebert, R. N. Faustov, and V. O. Galkin, “Mass spectra and Regge trajectories of light mesons in the relativistic quark model,” *Phys. Rev. D* **79** (2009) 114029, [arXiv:0903.5183 \[hep-ph\]](#).
- [21] S. Capstick and N. Isgur, “Baryons in a Relativized Quark Model with Chromodynamics,” *AIP Conf. Proc.* **132** (1985) 267–271.
- [22] G. Aarts, C. Allton, D. de Boni, S. Hands, B. Jäger, C. Praki, and J.-I. Skullerud, “Baryons in the plasma: in-medium effects and parity doubling,” *EPJ Web Conf.* **171** (2018) 14005, [arXiv:1710.00566 \[hep-lat\]](#).
- [23] G. Aarts, C. Allton, D. De Boni, S. Hands, B. Jäger, C. Praki, and J.-I. Skullerud, “Light baryons below and above the deconfinement transition: medium effects and parity doubling,” *JHEP* **06** (2017) 034, [arXiv:1703.09246 \[hep-lat\]](#).
- [24] R. Rapp and J. Wambach, “Chiral symmetry restoration and dileptons in relativistic heavy ion collisions,” *Adv. Nucl. Phys.* **25** (2000) 1, [arXiv:hep-ph/9909229](#).
- [25] W. Florkowski and W. Broniowski, “In-medium modifications of hadron masses and chemical freezeout in ultrarelativistic heavy ion collisions,” *Phys. Lett. B* **477** (2000) 73–76, [arXiv:nucl-th/9910016](#).
- [26] M. Michalec, W. Florkowski, and W. Broniowski, “Scaling of hadron masses and widths in thermal models for ultrarelativistic heavy ion collisions,” *Phys. Lett. B* **520** (2001) 213–216, [arXiv:nucl-th/0103029](#).

- [27] M. Bluhm, M. Nahrgang, and J. M. Pawłowski, “Locating the freeze-out curve in heavy-ion collisions,” [arXiv:2004.08608](#) [[nucl-th](#)].
- [28] Y. Aoki, G. Endrodi, Z. Fodor, S. Katz, and K. Szabo, “The Order of the quantum chromodynamics transition predicted by the standard model of particle physics,” *Nature* **443** (2006) 675–678, [arXiv:hep-lat/0611014](#).
- [29] A. Andronic, P. Braun-Munzinger, J. Stachel, and M. Winn, “Interacting hadron resonance gas meets lattice QCD,” *Phys. Lett. B* **718** (2012) 80–85, [arXiv:1201.0693](#) [[nucl-th](#)].
- [30] P. M. Lo, B. Friman, K. Redlich, and C. Sasaki, “S-matrix analysis of the baryon electric charge correlation,” *Phys. Lett. B* **778** (2018) 454–458, [arXiv:1710.02711](#) [[hep-ph](#)].
- [31] **ALICE** Collaboration, B. Abelev *et al.*, “Centrality dependence of  $\pi$ , K, p production in Pb-Pb collisions at  $\sqrt{s_{NN}} = 2.76$  TeV,” *Phys. Rev. C* **88** (2013) 044910, [arXiv:1303.0737](#) [[hep-ex](#)].
- [32] **ALICE** Collaboration, B. Abelev *et al.*, “ $K_S^0$  and  $\Lambda$  production in Pb-Pb collisions at  $\sqrt{s_{NN}} = 2.76$  TeV,” *Phys. Rev. Lett.* **111** (2013) 222301, [arXiv:1307.5530](#) [[nucl-ex](#)].
- [33] **ALICE** Collaboration, B. Abelev *et al.*, “Multi-strange baryon production at mid-rapidity in Pb-Pb collisions at  $\sqrt{s_{NN}} = 2.76$  TeV,” *Phys. Lett. B* **728** (2014) 216–227, [arXiv:1307.5543](#) [[nucl-ex](#)]. [Erratum: *Phys. Lett. B* **734** (2014) 409].
- [34] **ALICE** Collaboration, B. Abelev *et al.*, “ $K^*(892)^0$  and  $\phi(1020)$  production in Pb-Pb collisions at  $\sqrt{s_{NN}} = 2.76$  TeV,” *Phys. Rev. C* **91** (2015) 024609, [arXiv:1404.0495](#) [[nucl-ex](#)].
- [35] **ALICE** Collaboration, J. Adam *et al.*, “ ${}^3_{\Lambda}\text{H}$  and  ${}^3_{\Lambda}\bar{\text{H}}$  production in Pb-Pb collisions at  $\sqrt{s_{NN}} = 2.76$  TeV,” *Phys. Lett. B* **754** (2016) 360–372, [arXiv:1506.08453](#) [[nucl-ex](#)].
- [36] **ALICE** Collaboration, J. Adam *et al.*, “Production of light nuclei and anti-nuclei in pp and Pb-Pb collisions at energies available at the

- CERN Large Hadron Collider,” *Phys. Rev. C* **93** (2016) 024917, arXiv:1506.08951 [nucl-ex].
- [37] **ALICE** Collaboration, S. Acharya *et al.*, “Production of  ${}^4\text{He}$  and  ${}^4\overline{\text{He}}$  in Pb-Pb collisions at  $\sqrt{s_{\text{NN}}} = 2.76$  TeV at the LHC,” *Nucl. Phys. A* **971** (2018) 1–20, arXiv:1710.07531 [nucl-ex].
- [38] V. D. Burkert and C. D. Roberts, “Colloquium : Roper resonance: Toward a solution to the fifty year puzzle,” *Rev. Mod. Phys.* **91** (2019) 011003, arXiv:1710.02549 [nucl-ex].
- [39] A. Andronic, P. Braun-Munzinger, B. Friman, P. M. Lo, K. Redlich, and J. Stachel, “The thermal proton yield anomaly in Pb-Pb collisions at the LHC and its resolution,” *Phys. Lett. B* **792** (2019) 304–309, arXiv:1808.03102 [hep-ph].
- [40] P. M. Lo, “private communication,”.
- [41] P. Alba, R. Bellwied, M. Bluhm, V. Mantovani Sarti, M. Nahrgang, and C. Ratti, “Sensitivity of multiplicity fluctuations to freeze-out conditions in heavy ion collisions,” *Phys. Rev. C* **92** (2015) 064910, arXiv:1504.03262 [hep-ph].
- [42] R. Bellwied, “Sequential Strangeness Freeze-out,” *EPJ Web Conf.* **171** (2018) 02006, arXiv:1711.00514 [nucl-ex].
- [43] P. Braun-Munzinger, B. Friman, K. Redlich, A. Rustamov, and J. Stachel, “Relativistic nuclear collisions: Establishing the non-critical baseline for fluctuation measurements,” arXiv:2007.02463 [nucl-th].